

ADVANCED MATERIALS

Supporting Information

for *Adv. Mater.*, DOI: 10.1002/adma.202103660

A Universal Approach for Room-Temperature Printing
and Coating of 2D Materials

*Sina Abdolhosseinzadeh, Chuanfang (John) Zhang,
René Schneider, Mahdiah Shakoorioskooie, Frank
Nüesch, and Jakob Heier**

Supplementary Information

A Universal Approach for Room-temperature Printing and Coating of Two-dimensional Materials

Sina Abdolhosseinzadeh^{1,2}, Chuanfang (John) Zhang¹, René Schneider¹, Mahdiah
Shakoorioskooie^{1,3}, Frank Nüesch^{1,2}, Jakob Heier¹ *

¹ Swiss Federal Laboratories for Materials Science and Technology (Empa), Dübendorf, Switzerland

² Institute of Materials Science and Engineering, Swiss Federal Institute of Technology Lausanne (EPFL), Lausanne, Switzerland

³ Institute for Building Materials, Swiss Federal Institute of Technology Zürich (ETHZ), Zürich, Switzerland

* Corresponding author (jakob.heier@empa.ch)

Materials and Methods:

Table 1. List of utilized materials.

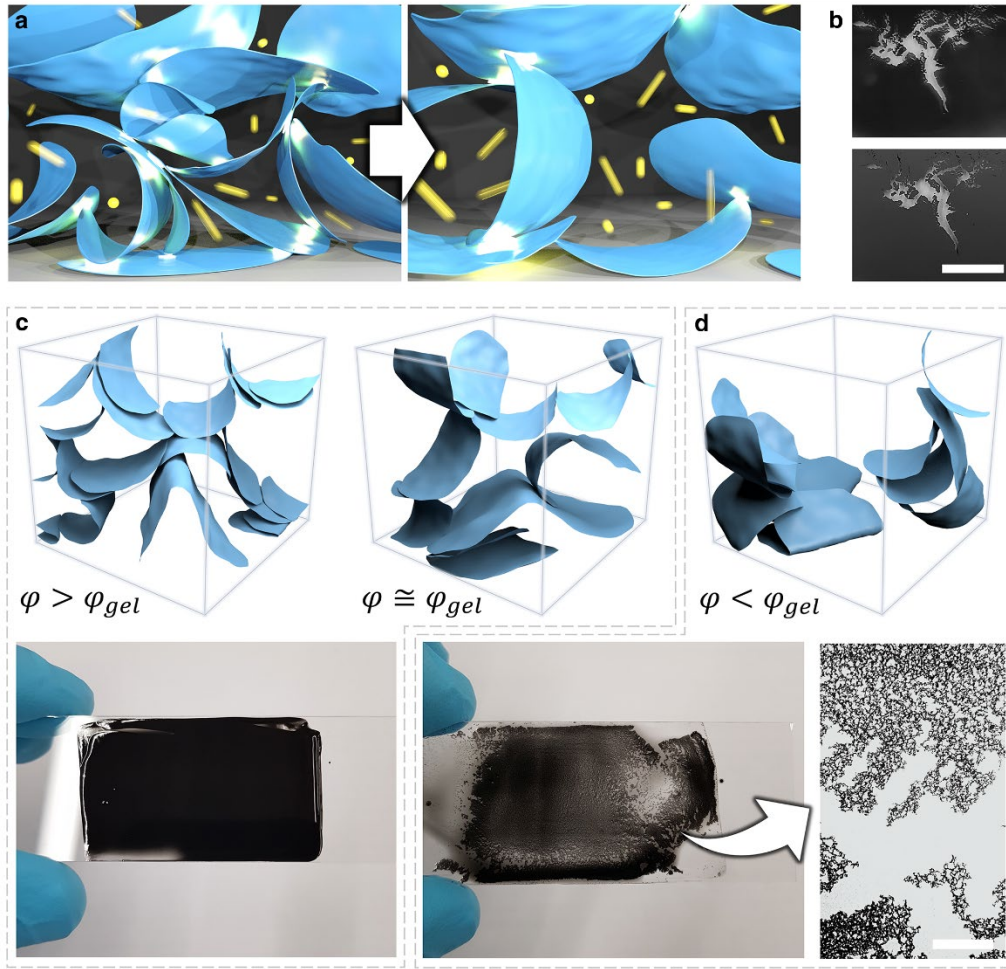
#	Material	Manufacturer	Product code
1	Graphite	Sigma Aldrich	332461
2	WSe ₂	Alfa Aesar	13084.09
3	WS ₂	Sigma Aldrich	243639
4	MoSe ₂	Sigma Aldrich	778087
5	MoS ₂	Sigma Aldrich	69860
6	InSe	Ossila	M2135C1
7	SnS	Sigma Aldrich	741000
8	Single-walled carbon nanotube (SWCNT)	Sigma Aldrich	805033
9	Multi-walled carbon nanotube (MWCNT)	Ossila	M2008D1
10	Zinc oxide nanowires (ZnO NWs)	ACS Materials	NWZO01A5
11	Titanium dioxide nanotubes (TiO ₂ NTs)	Sigma Aldrich	799289
12	Carbon black nanoparticles	Solaronix	
13	Zinc oxide nanoparticles (ZnO NPs 18 nm)	US Research Nanomaterials	US3599
14	Zinc oxide nanoparticles (ZnO NPs 100 nm)	Sigma Aldrich	721077
15	Zinc oxide nanoparticles (ZnO NPs 500 nm)	US Research Nanomaterials	US1003M-500 nm
16	Zinc oxide microparticles (ZnO NPs 10 µm)	US Research Nanomaterials	US1003M-10 µm
17	Indium tin oxide (ITO)	Sigma Aldrich	544876
18	Antimony tin oxide (ATO)	Sigma Aldrich	549541
19	Aluminium doped zinc oxide (AZO)	US Research Nanomaterials	US3805
20	Laponite clay	BYK	LAPONITE-EP
21	1-Ethyl-3-methylimidazolium bis(trifluoromethylsulfonyl)imide (EMIM-TFSI)	Iolitec	
22	Poly-(vinylidenfluorid-co-hexafluorpropylen) (PVDF-HFP)	Sigma Aldrich	427187

Instruments and characterization methods:

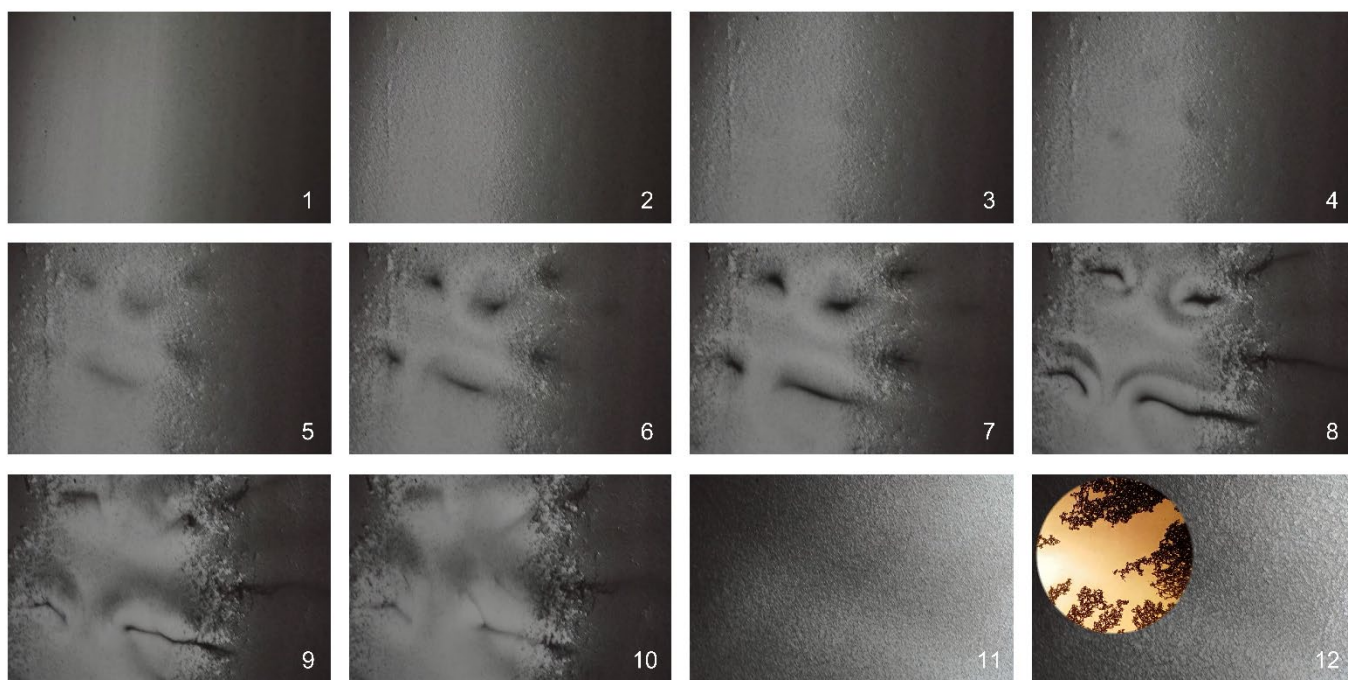
The rheological characterizations were carried out by an Anton Paar MCR 301 rheometer with a 25 mm profiled parallel plate (PP25/P2) measuring system. All the tests were performed at 25°C, with a gap size of 1 mm. Examination of the “low-shear-treatment” process was done by 25 mm flat parallel plate measurement system at a gap distance of 100 µm. The X-ray tomography was performed using an EasyTomo XL-Ultra tomograph (RX Solutions) with a cone-beam geometry. The X-ray source (Hamamatsu L10711-02) was equipped with a LaB₆ filament and a 1 µm-thick W target deposited on a 500 nm-thick diamond support, which allowed achieving sub-micron X-ray source focal spot size. For each tomography, 3600 radiographs were acquired over 360° of specimen rotation. Tomogram reconstruction was carried out using a GPU-optimized cone beam filtered back-projection algorithm provided by RX Solutions (XACT Ver. 1.1). The effective spatial resolution in the tomograms were approximately 1.92 µm and 2.78 µm for DME and freeze-dried vdW ink, respectively. The DC characteristics of the electrolyte-gated field-effect transistor were

acquired in the dark with a Keithley 4200 Semiconductor parameter analyser. Cyclic voltammetry tests were performed on a μ Autolab type III with a platinum wire as a pseudo-reference electrode.

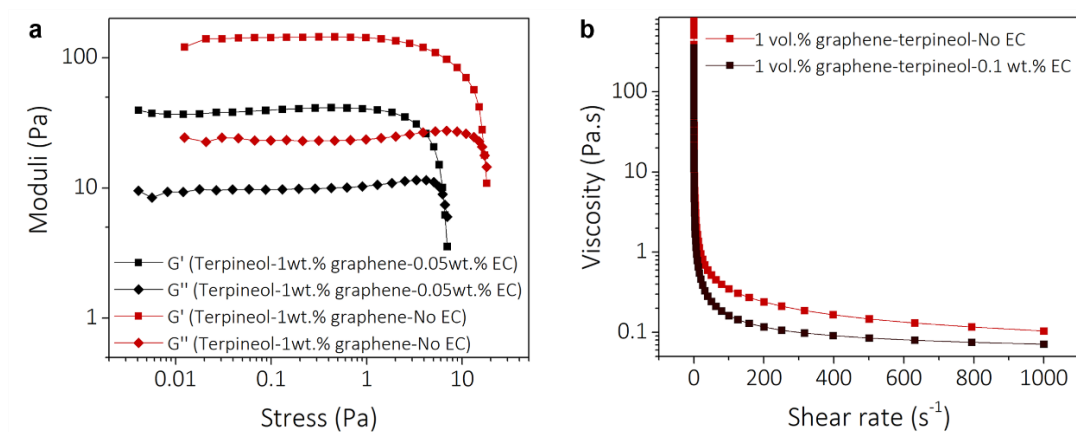
The microstructures and exfoliated particles were characterized by Scanning Electron Microscopy (SEM, FEI NanoSEM 230), Atomic Force Microscopy (AFM, Bruker ICON3), and Transmission Electron Microscopy (bright field imaging TEM with 200 kV using JEOL 2200 FS). Slot die coating was done on a TSE Troller (Switzerland) tabletop slot die coater. Screen-, gravure-, and flexographic-printing were performed on a C600 multifunctional printer (nsm Norbert Schläfli). Extrusion-printing was done using a direct ink writing equipment from EnvisionTEC (Bioplotter Manufacturing Series). An AJ 5X System (Optomec) with a pneumatic atomizer was used for aerosoljet printing.



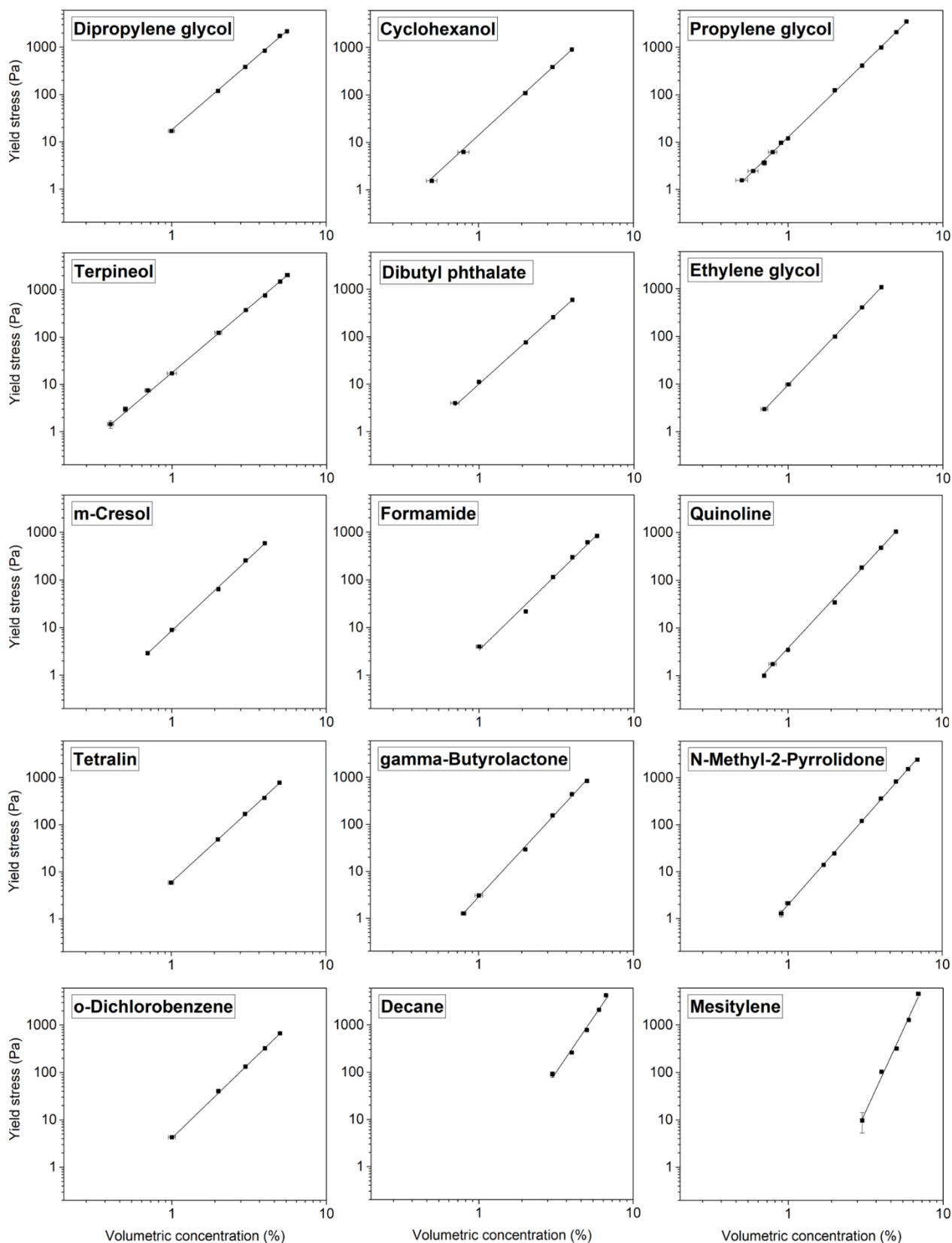
Supplementary Fig. 1. (a) Schematic illustration of a vdW ink before (left) and after dilution (right). (b) Formation of cracks in a wet film (top) made with a terpeneol-graphene vdW ink $\varphi \cong \varphi_{gel}$ (bottom: after drying; scale bar: 7 mm). (c) Aggregated dispersions with compositions above gel point ($\varphi \geq \varphi_{gel}$) can form continuous films. (d) In aggregated dispersions with compositions below gel point ($\varphi < \varphi_{gel}$) phase separation occurs, and a continuous film cannot be obtained (scale bar: 100 μm).



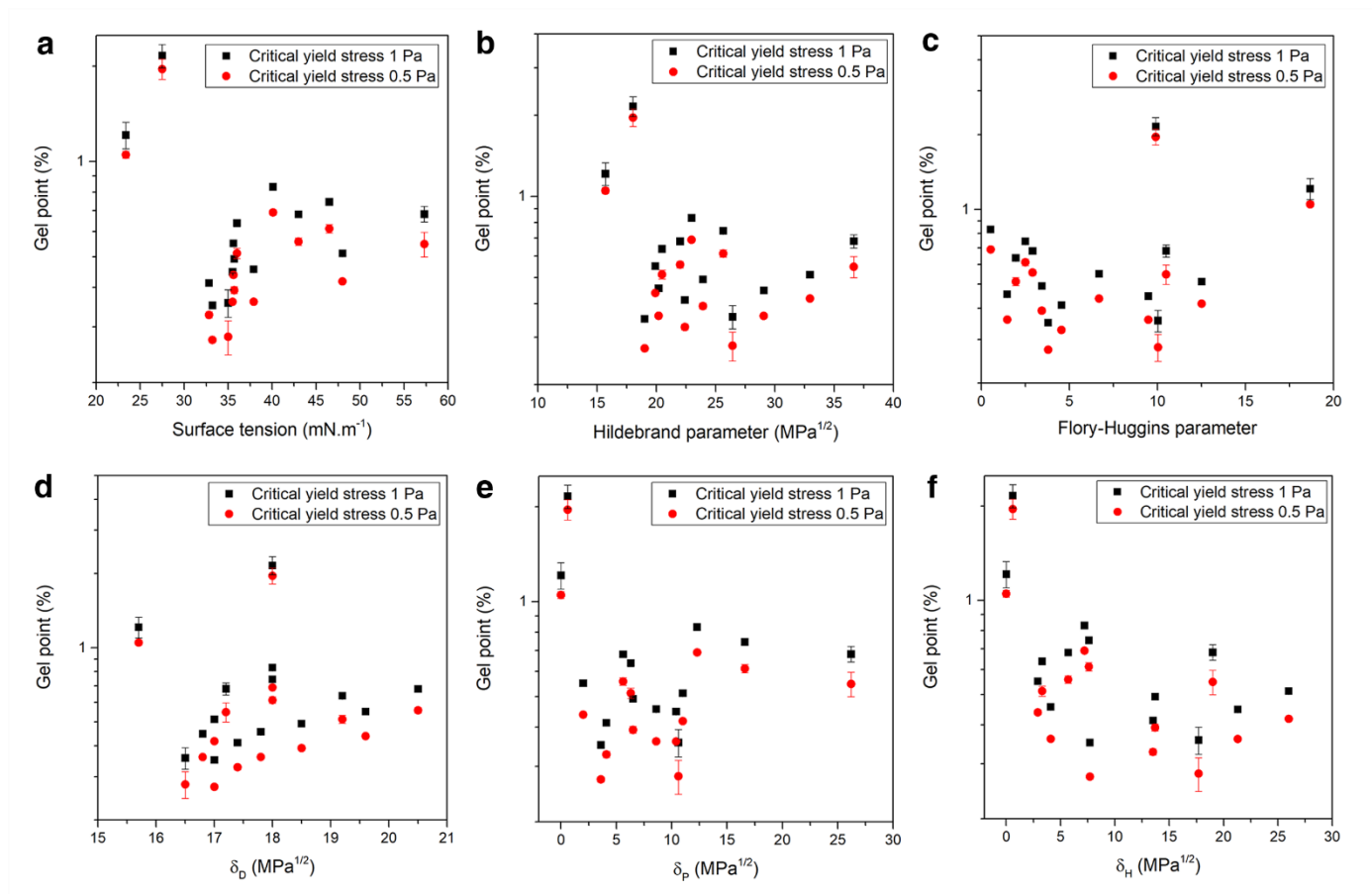
Supplementary Fig. 2. Occurrence of phase separation after addition of a drop of solvent to a film made with a graphene vdW gel. In image 1 (the drop is not added yet). Images 2-10 show the time-dependent evolutions. Image 11 shows the diluted ink after homogenization. Image 12: since the composition of the dispersion is below the gel point, gel formation is not possible (even after homogenization).



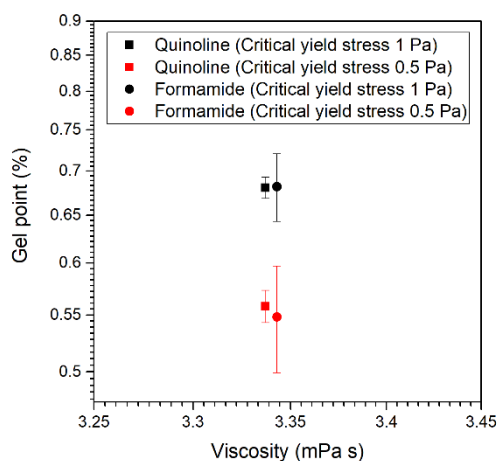
Supplementary Fig. 3. Effect of addition of a binder (ethyl cellulose) to a terpeneol-graphene vdW ink on its (a) yield strength (amplitude sweep test results) and (b) viscosity.



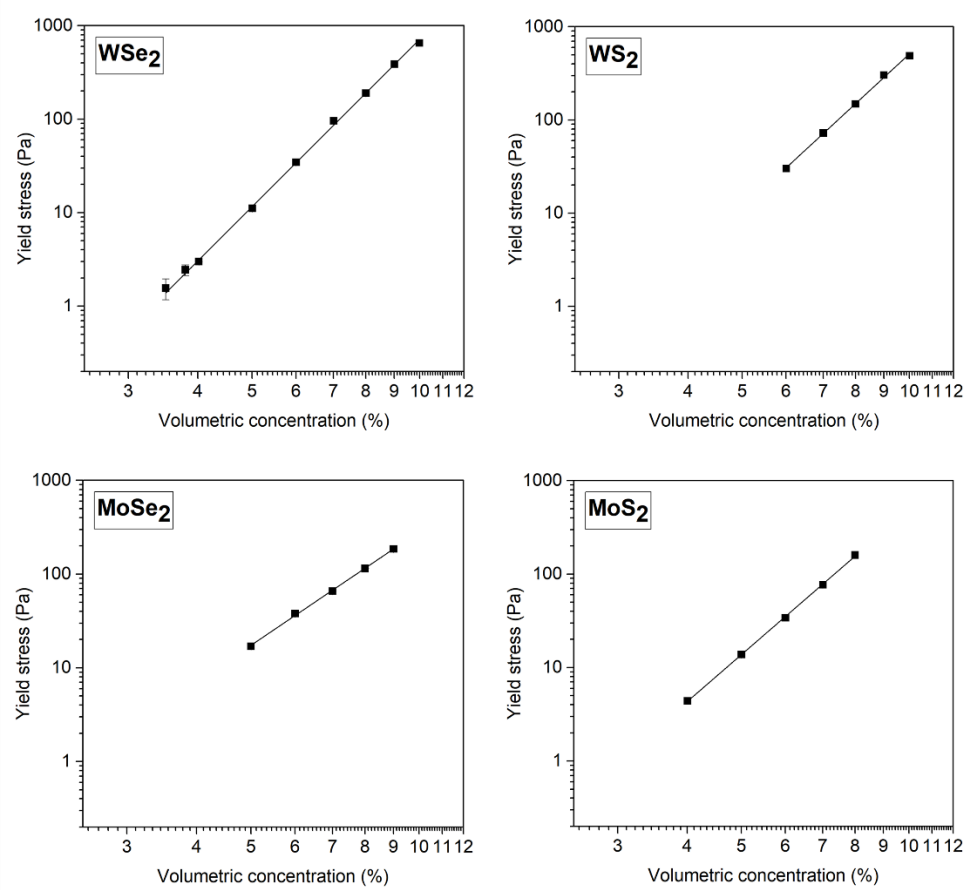
Supplementary Fig. 4. Power-law relationship between yield strength of graphene gels (vdW inks) and volumetric concentration of graphene in different solvents.



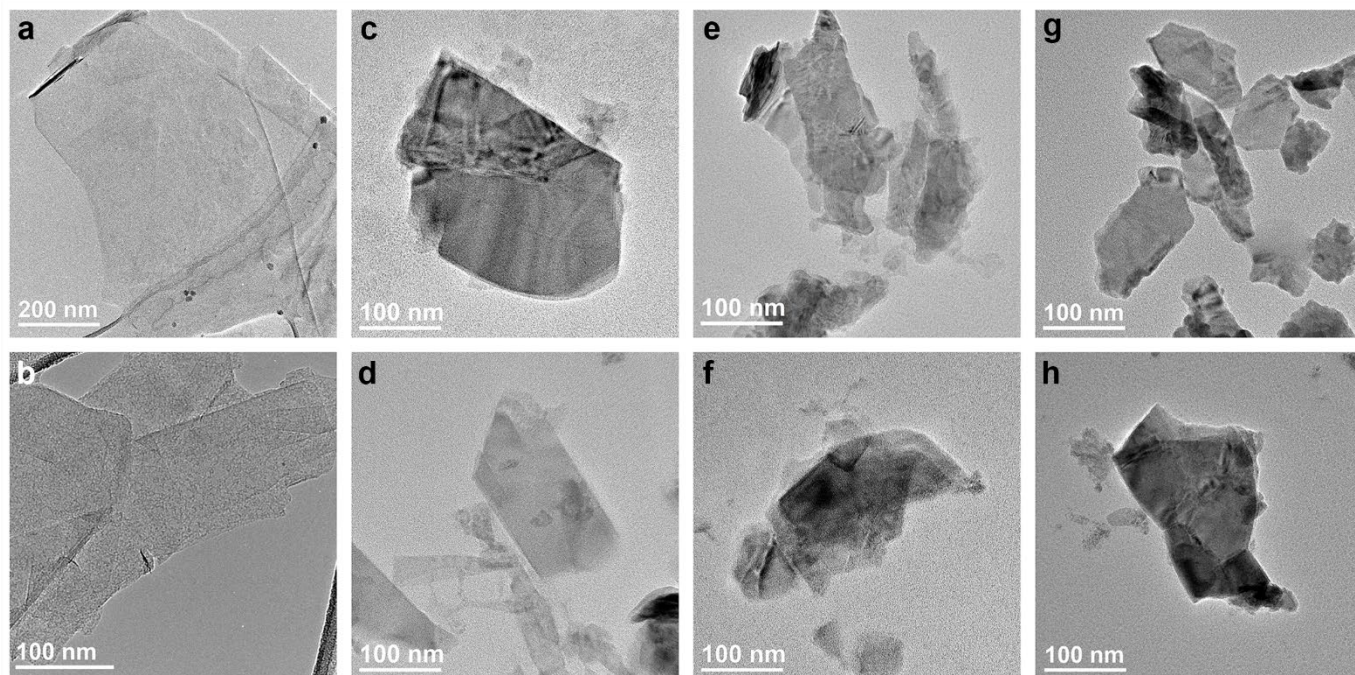
Supplementary Fig. 5. Relationship between critical volumetric concentration (ϕ_{gel}) of graphene gels and (a) surface tension, (b) Hildebrand parameter, (c) Flory-Huggins parameter, and (d-f) Hansen solubility parameters of the utilized solvents.



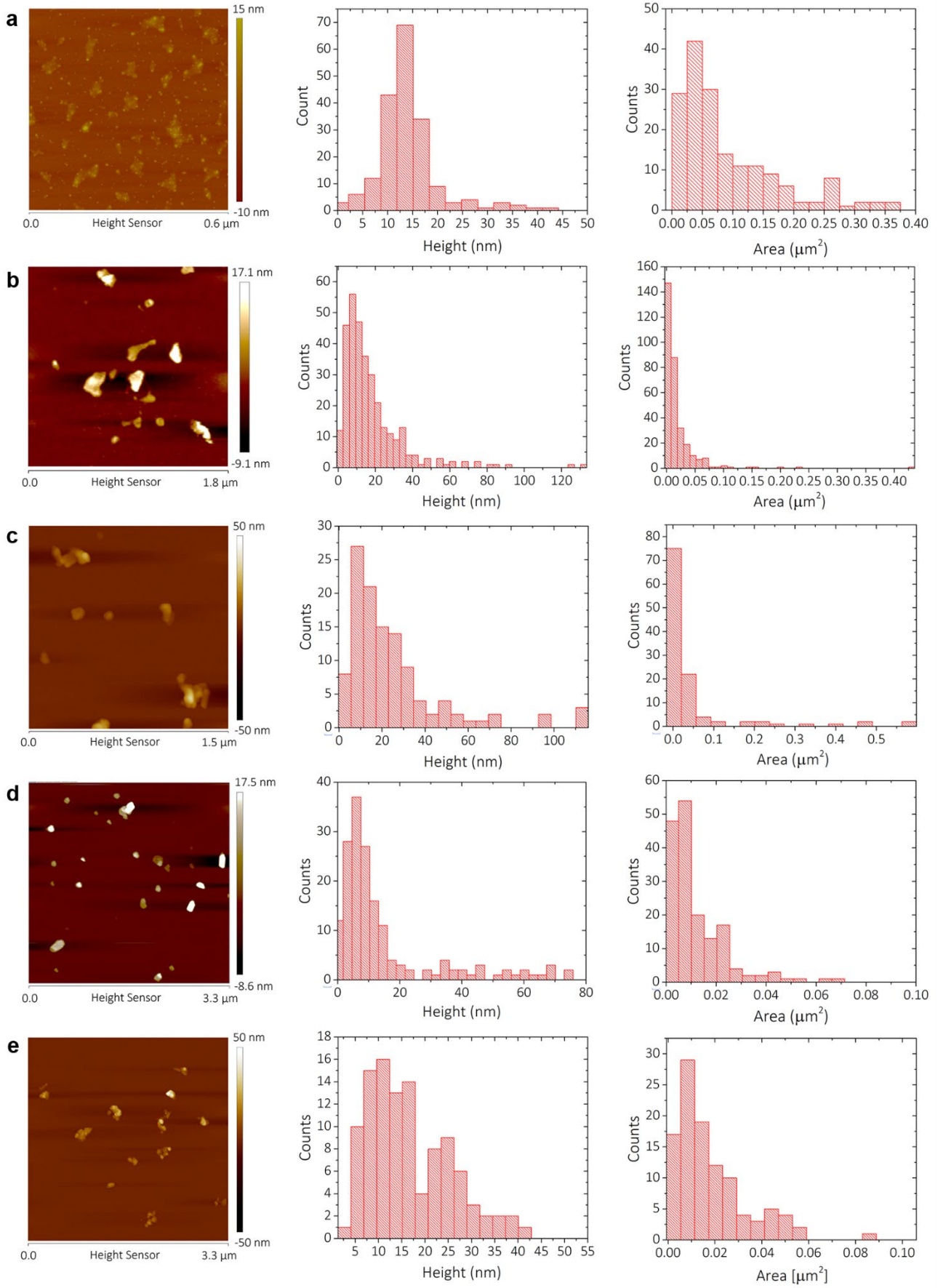
Supplementary Fig. 6. Relationship between critical volumetric concentration (ϕ_{gel}) and utilized solvent viscosity of two graphene gels made with quinoline and formamide.



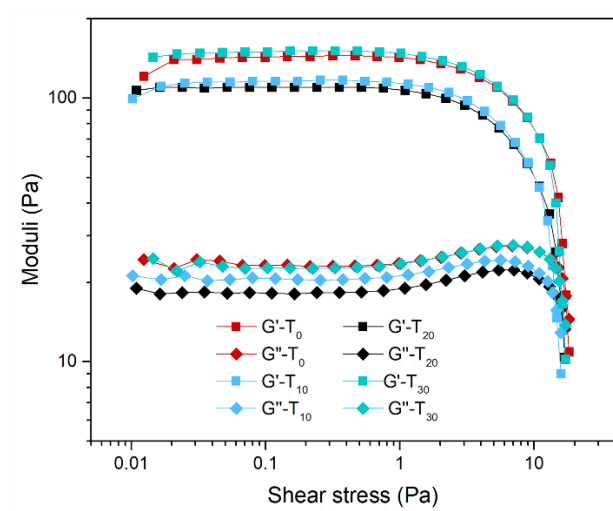
Supplementary Fig. 7. Power-law relationship between yield strength of vdW gels and volumetric concentration of 2D material in NMP.



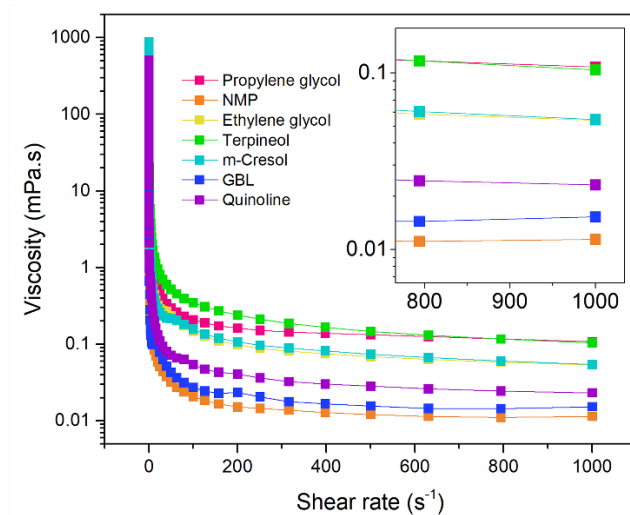
Supplementary Fig. 8. Transmission electron microscopy images of exfoliated (a) graphene, (b) RGO, (c) WSe₂, (d) WS₂, (e) MoSe₂, (f) MoS₂, (g) InSe, (h) SnS.



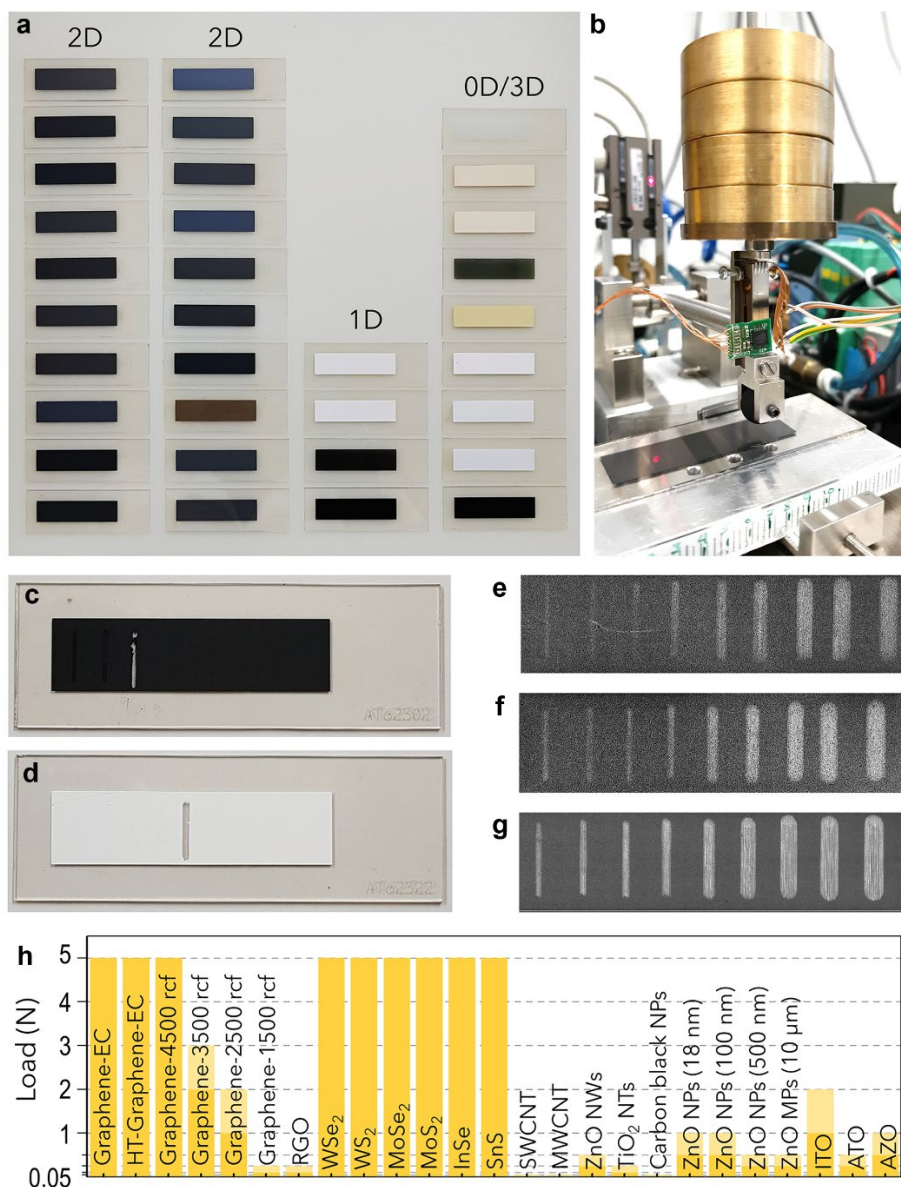
Supplementary Fig. 9. Atomic force microscopy images of exfoliated (a) graphene, (b) MoS₂, (c) MoSe₂, (d) WS₂, (e) WSe₂.



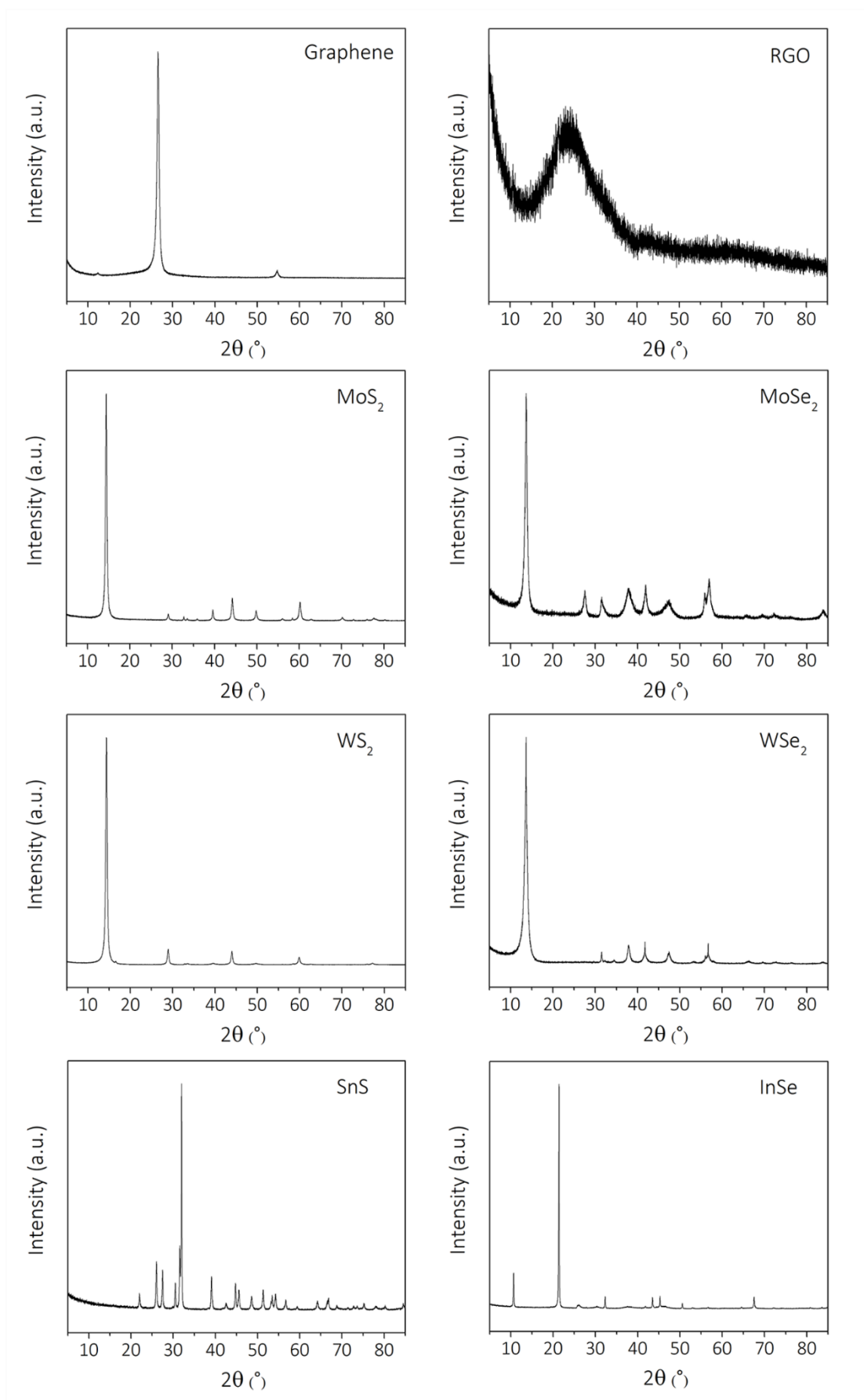
Supplementary Fig. 10. Temporal amplitude sweep tests of a single graphene vdW ink: T_0 : as-prepared, T_{10} : after 10 days, T_{20} : after 20 days, and T_{30} : after 30 days.



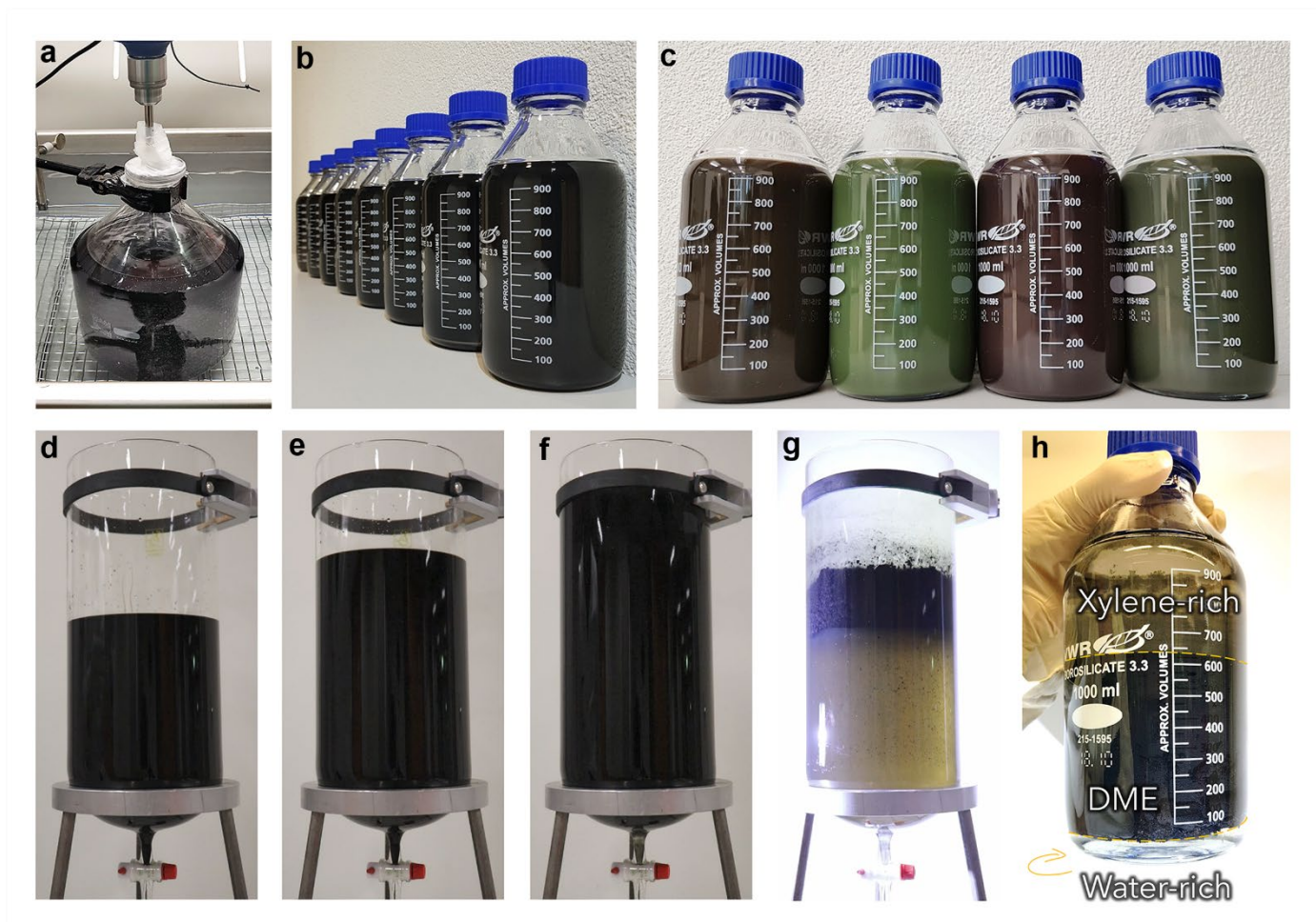
Supplementary Fig. 11. Dependence of the viscosity of graphene vdW inks (with similar volume fractions) on the utilized solvent.



Supplementary Fig. 12. Digital photographs of (a) blade coated films made with additive-free gels of different types of nanomaterials, (b) abrasive wear test, (c-d) two examples of abrasive wear test specimens after failure (c: RGO and d: ZnO NPs 500nm). Optical microscopy images of abrasive wear test specimens (e) Graphene-EC, (f) HT-Graphene-EC, and (g) Graphene-4500 rcf (when films withstood the maximum applied force, wear test profiles were compared). (h) Abrasive wear test results for films made with additive-free gels of different types of nanomaterials (Graphene-EC: ethylcellulose-containing graphene ink before heat treatment, HT-Graphene-EC: ethylcellulose-containing graphene ink heat-treated at 300°C for 1h, Graphene-4500 rcf: graphene vdW ink made with graphene suspension centrifuged at 4500 rcf, Graphene-3500 rcf: graphene gel made with graphene suspension centrifuged at 3500 rcf, Graphene-2500 rcf: graphene gel made with graphene suspension centrifuged at 2500 rcf, Graphene-1500 rcf: graphene gel made with graphene suspension centrifuged at 1500 rcf). Gels of other nanomaterials were also made with the same procedure as vdW inks, by dispersing them in NMP, removing nondispersed particles, extraction of well-dispersed particles by IAE method and transferring them to small amount of NMP to form a gel ($\varphi \geq \varphi_{gel}$). All of the films were coated with similar thicknesses ($\sim 4 \mu\text{m}$) by adjusting the thickness of the wet films (depending on the solid content of the gels).



Supplementary Fig. 13. X-ray diffraction patterns of 2D materials films coated on glass substrates from gel inks (all vdW inks except for RGO).



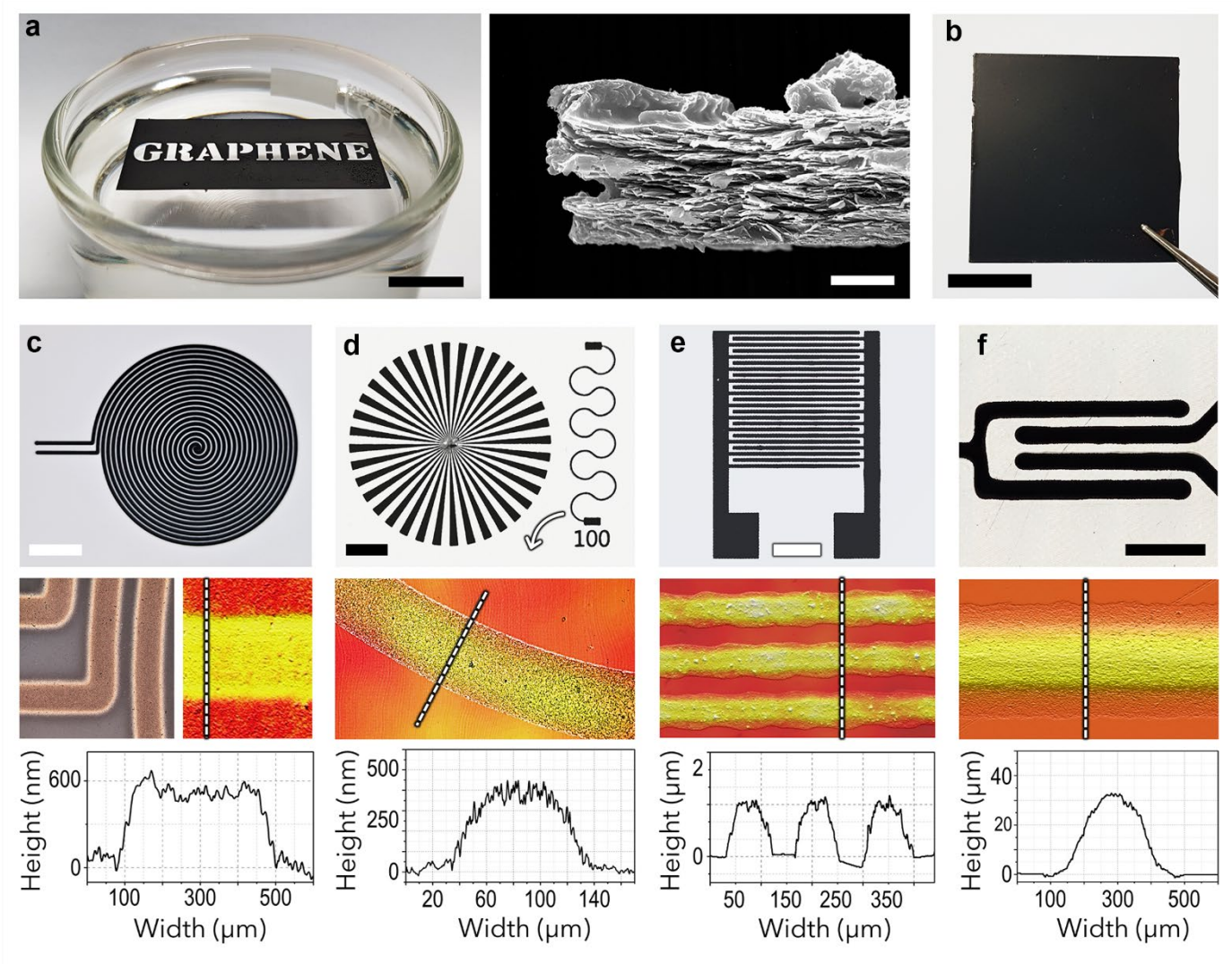
Supplementary Fig. 14. Large scale exfoliation of 2D materials (a) bath sonication of 5L graphene dispersion, (b) graphene suspensions in NMP, (c) From left to right: MoSe₂ (in NMP), MoS₂ (in Water/IPA), WSe₂ (in NMP), WS₂ (in Water/IPA) suspensions. (d-h) Consecutive steps of interface-assisted extraction method for processing 3L of graphene-NMP suspension (d) addition of graphene-NMP suspension to the separation funnel, (e) addition of xylene, (f) addition of water, (g) phase separation (completed in a few seconds), (h) graphene concentrate is collected for further processing.

Table 2. Minimum water content for initiation of the phase separation.

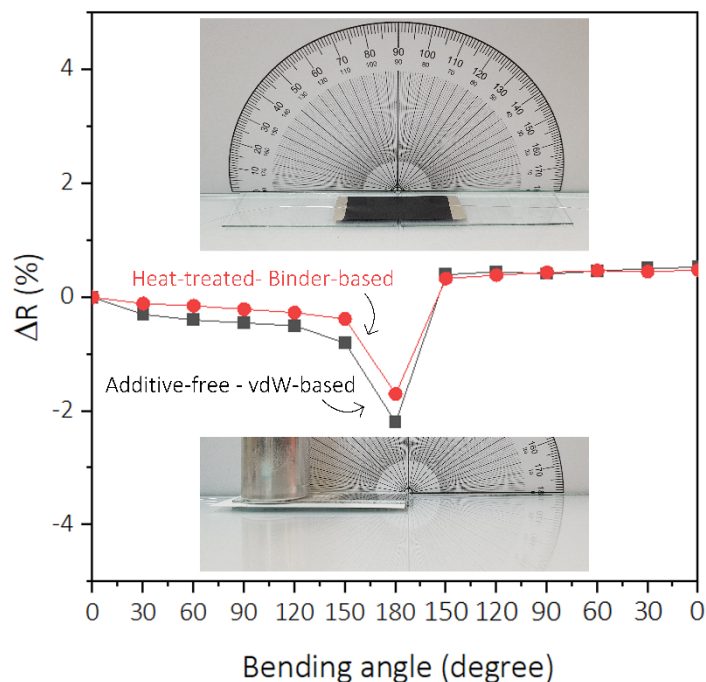
Dispersion solvent (S ₁)	Water-immiscible solvent (S ₂)	Minimum critical ratio (S ₁ /S ₂ /H ₂ O)
NMP	Toluene	1/1/0.2
NMP	Butyl acetate	1/1/0.24
NMP	Propyl acetate	1/1/0.36
NMP	Amyl acetate	1/1/0.18
NMP	Xylene	1/1/0.15
NMP	Cyclohexane	1/1/0.065
NMP	Anisole	1/1/0.38



Supplementary Fig. 15. Digital photographs of a deep-metastable-emulsion of graphene (water-NMP-xylene system) after centrifugation at 12500 ref.



Supplementary Fig. 16. (a) Left: A free-standing graphene film floating on the surface of formamide. A 1.7 vol.% NMP-graphene vdW ink ($\tau_y = 14 \text{ Pa}$) is blade coated (laser-scribed for patterning) on glass and separated (from it) by placing a few drops of formamide close to the edges of the film (on the glass). Such a film can also be used for conformal printing of 2D materials (scale bar: 2 cm). Right: SEM image of the same free-standing film (scale bar: 1 μm). (b) Spin-coated MoSe₂ film on a glass substrate from a 3 vol.% NMP-MoSe₂ vdW ink ($\tau_y = 2 \text{ Pa}$). Hot air (50°C) was used to speed-up the drying upon spinning (scale bar: 1 cm). (c) Aerosoljet printed (with a pneumatic atomizer) terpineol-graphene vdW ink (0.5 vol.%, $\tau_y = 3 \text{ Pa}$) on a glossy photopaper and corresponding height profiles (scale bar: 3 mm). (d) Flexographic printing of a 0.7 vol.% terpineol (80 vol.):IPA (20 vol.%) -graphene vdW ink ($\tau_y \cong 2 \text{ Pa}$) on glossy photopaper and corresponding height profiles (scale bar: 3 mm) (e) Screen printed 2 vol.% terpineol-graphene vdW ink on a glossy photopaper ($\tau_y = 120 \text{ Pa}$) and corresponding height profiles (scale bar: 1.5 mm) (f) Extrusion printed 8 vol.% NMP-WSe₂ vdW ink on a PET substrate and corresponding height profiles (scale bar: 2mm).

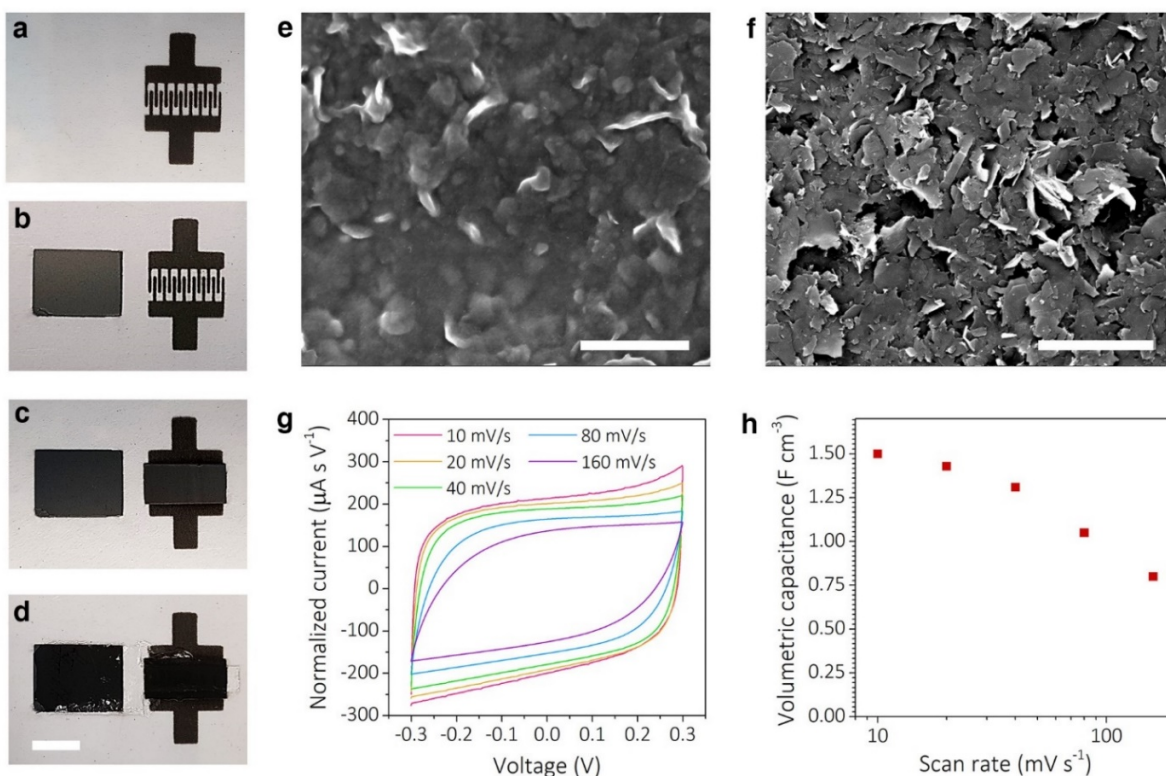


Supplementary Fig. 17. Resistance change as a function of bending angle in additive-free and additive-containing films (after heat-treatment).

Supplementary note 1

Printing and characterization of the electrolyte-gated field-effect transistor:

A propylene glycol-graphene vdW ink (4 wt.% graphene) was used for screen-printing the source, drain and gate electrodes on a PET substrate. To print the source and drain, small amount of laponite clay (0.04 wt.%) was added to the ink to reduce the porosity of the films ($L = 200 \mu\text{m}$, $W = 3\text{cm}$). For this purpose, the clay was first dissolved in DI water with a concentration of 1 wt.%. The active layer (WSe_2) was screen-printed from an NMP- WSe_2 vdW ink (8 vol.% WSe_2). Gel electrolyte was inkjet printed from a solution of EMIM-TFSI/PVDF-HFP in acetone-dimethylacetamide mixture (weight ratio EMIM-TFSI:PVDF-HFP:acetone:dimethylacetamide = 2.5:1:4.5:3.5). The whole fabrication process was carried out under ambient conditions.



Supplementary Fig. 18. (a-d) Consecutive steps of printing an electrolyte gated field-effect transistor (scale bar: 6 mm). (a) Screen printed source and drain interdigitated electrodes from a propylene glycol-graphene vdW ink (4wt.% graphene, 0.04 wt.% laponite clay). (b) Screen printed (5 passes) gate electrode from a propylene glycol-graphene vdW ink (4wt.%). (c) Screen printed active layer from an NMP-WSe₂ vdW ink (8 vol.%). (d) Inkjet printed electrolyte from a solution of EMIM-TFSI/PVDF-HFP in an acetone-dimethylacetamide mixture. (e, f) SEM images of the surface of a (e) laponite-containing graphene film (used for printing the source and drain electrodes; scale bar: 2 μm), and a (f) laponite-free graphene film (used for printing the gate electrode; scale bar: 2 μm). (g) Normalized cyclic voltammetry results for determination of capacitance at electrolyte-active layer interface (voltage vs. pseudo-reference electrode). (h) Volumetric capacitance of the transistor channel at different scan rates.